

Supporting Information for

Origin of Shielding and Deshielding Effects in NMR Spectra of Organic Conjugated Polyynes

Andreas Ehnbom,[●] Michael B. Hall,^{●*} and John A. Gladysz^{●*}

Department of Chemistry, Texas A&M University, PO Box 30012, College Station, Texas
77843-3012, USA

1. Computational Details

The general computational methodology employed is outlined in Figure s1. First, validation methods were sought to ensure the accuracy of the results. A variety of functionals were compared by building diterminal conjugated polyynes $H(C\equiv C)_nH$ ($n = 2-10$). For the starting geometries, C–C and C≡C bond lengths of 1.54 Å and 1.22 Å were used. Metrical parameters from crystal structures were not employed as non-biased distances were desired for evaluating the functionals. Although the input structures possessed $D_{\infty h}$ symmetry, no constraints were applied in the calculations. The structures were optimized using each of the following functionals: BMK,^{s1} M06,^{s2} CAM-B3LYP,^{s3} ωB97XD,^{s4} PBE0,^{s5} B3LYP,^{s6} M06L,^{s7} BLYP,^{s6a,c} and BP86.^{s6a,s8} In all cases, a triple-zeta Pople basis set [6-311++G(d,p)]^{s9} that has extra diffuse and polarization functions was used. All computations were performed with the Gaussian09 program package, employing the ultrafine grid (99,590) to enhance accuracy.^{s10}

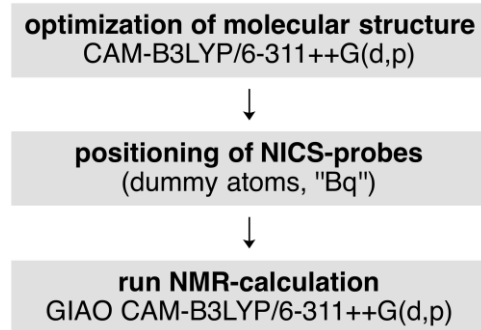


Figure s1. Graphical outline of the calculation sequence.

Results for the octayne $H(C\equiv C)_8H$ were compared with the crystal structure of *t*-Bu-(C≡C)₈*t*-Bu (CCSD code LUMWAS).^{s11} Table s1 summarizes, for each functional, the *sum* of (1) the percent difference in the average C–C bond lengths, and (2) the percent difference in the average C≡C bond lengths. The underlying data are presented in Table s2. The CAM-B3LYP functional performed well (ranking second) and was used for subsequent calculations as it has been extensively employed for accurate NMR simulations.^{s12} The basis sets were then evaluated [6-311++G(d,p),^{s9} 6-311+G(d),^{s9} 6-311+G,^{s9} and 6-31+G(d)^{s13} in order of decreasing quality], and representative data are given in Table s3. The choice of basis set had little influence upon the NICS values (or bond lengths) unless they were small relative to the maximum values. This is al-

so supported in related studies.^{s14} However, it is important to use polarization functions and diffuse functions when computing NMR chemical shifts, so the best quality basis set (triple zeta) was used [6-311++G(d,p)].^{s9} The functionals were also evaluated on the basis of their NICS values, but no significant difference was observed (Table s4). Importantly, in accord with the sign convention for NICS, the sign was inverted on values from the isotropic portion of the data.^{s15}

Table s1. The sum of (1) the percent difference in average C-C bond lengths, and (2) the percent difference in average C=C bond lengths for those in the crystal structure of *t*-Bu(C≡C)₈*t*-Bu^{s11} versus those computed for H(C≡C)₈H with various functionals.

functional	% difference ^a
ωB97XD	0.19
CAM-B3LYP	0.31
BMK	0.50
M06	1.20
PBE0	1.97
B3LYP	2.15
M06L	3.46
BLYP	4.14
BP86	4.37

^a This quantity is defined in the text and caption.

In addition to choosing an appropriate functional and basis set as described above, our methodology was also benchmarked versus two literature reports that produced NICS values. The first involved the classical example of benzene,^{s15} and Figure s2 (first and second panels) depicts the high level of agreement. The second involved a cyclic conjugated heptayne,^{s16} again with excellent agreement (Figure s2, third and fourth panels).

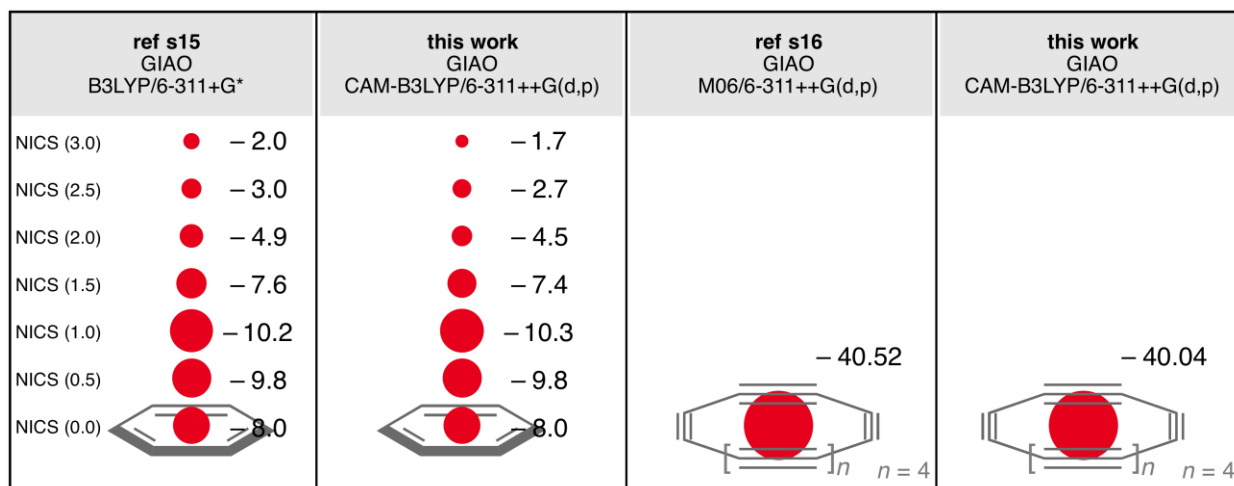


Figure s2. Validation of the computational methods: benchmarking vs. literature results.

Procedure for Figures s4-a-e. The diterminal conjugated polyynes were aligned with the x axis, such that the y coordinate for any carbon or hydrogen atom was zero (see Figure s3). NICS probes were positioned with the same x/y coordinates as the center of each carbon and hydrogen atom (see Table s5 for the bond lengths employed). For each value of x , additional probes were placed at y values of 0.5, 1.0, 1.5, 2.0, 2.5, and 3.0 Å. For each y value, additional NICS probes were extended beyond the terminal carbon atoms at values of 2.0, 2.5, and 3.0 Å. In view of the $D_{\infty h}$ symmetries of these molecules, data points are depicted for only half of each structure (regions thus omitted are marked with "×"). The computed values for all compounds are shown in Figures s4-a-e. Table s6 summarizes the computed bond lengths that in turn define the x values on the NICS grid. Both the optimized structures and the input files containing the NICS probes and their placement are provided as .xyz files.

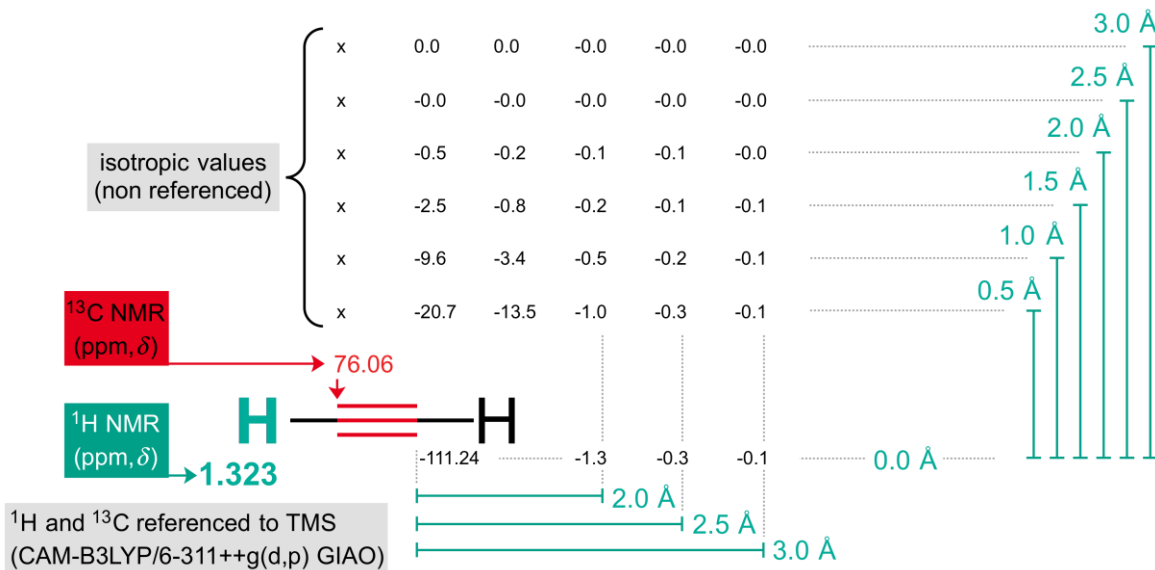


Figure s3. Graphical depiction of the different distances typically used in the NICS grid plots.

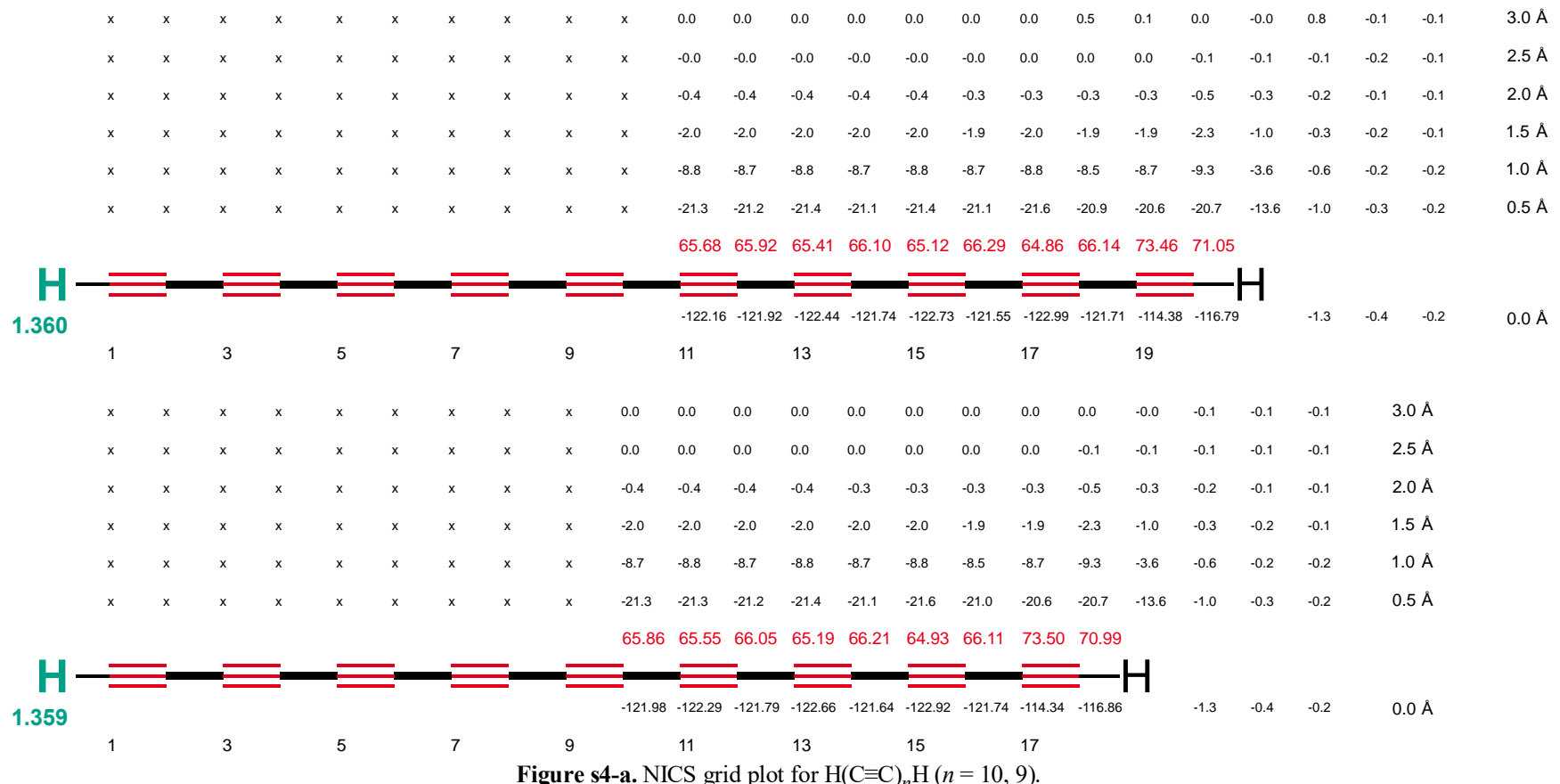


Figure s4-a. NICS grid plot for $\text{H}(\text{C}\equiv\text{C})_n\text{H}$ ($n = 10, 9$).

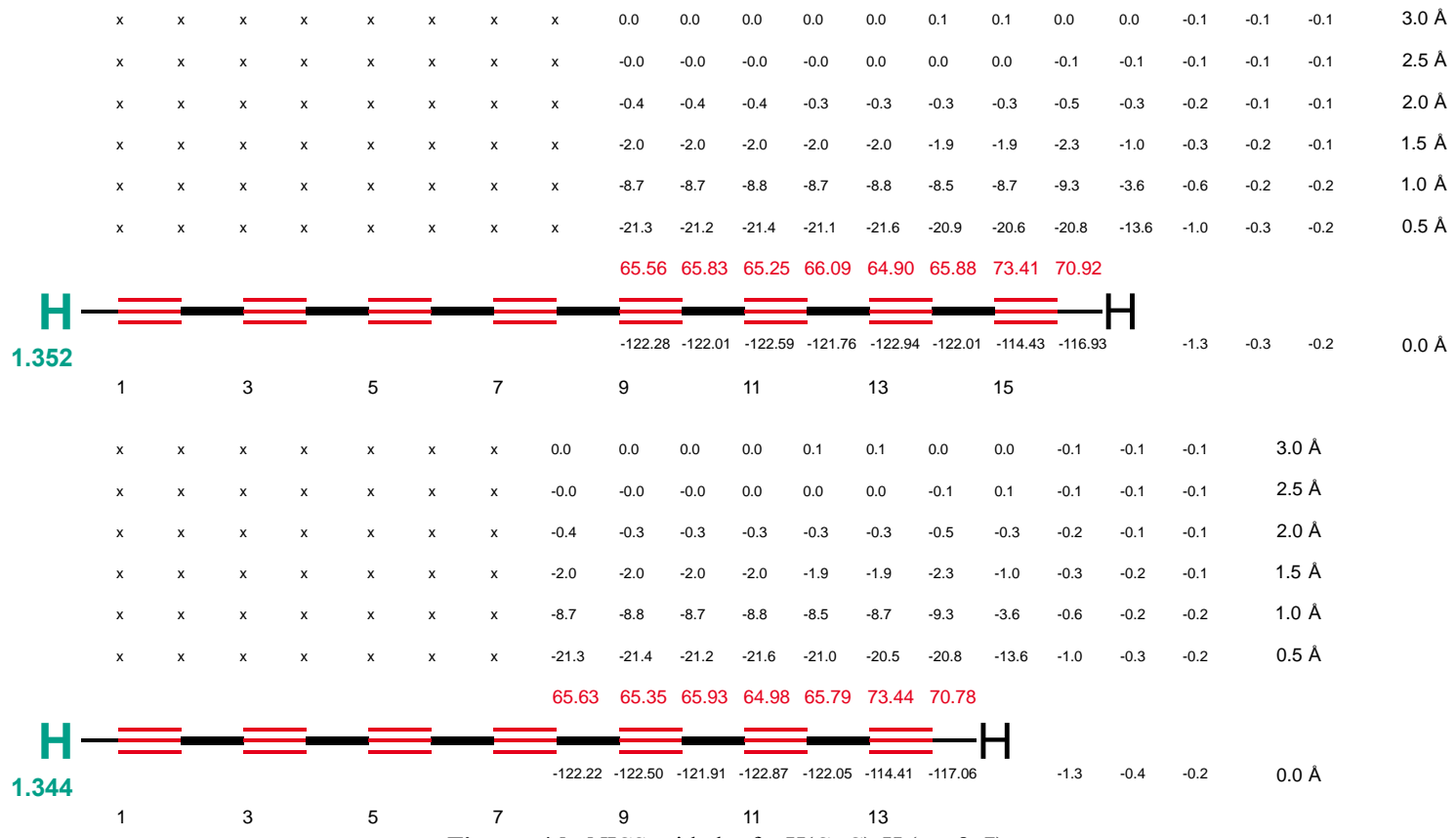


Figure s4-b. NICS grid plot for $\text{H}(\text{C}\equiv\text{C})_n\text{H}$ ($n = 8, 7$).

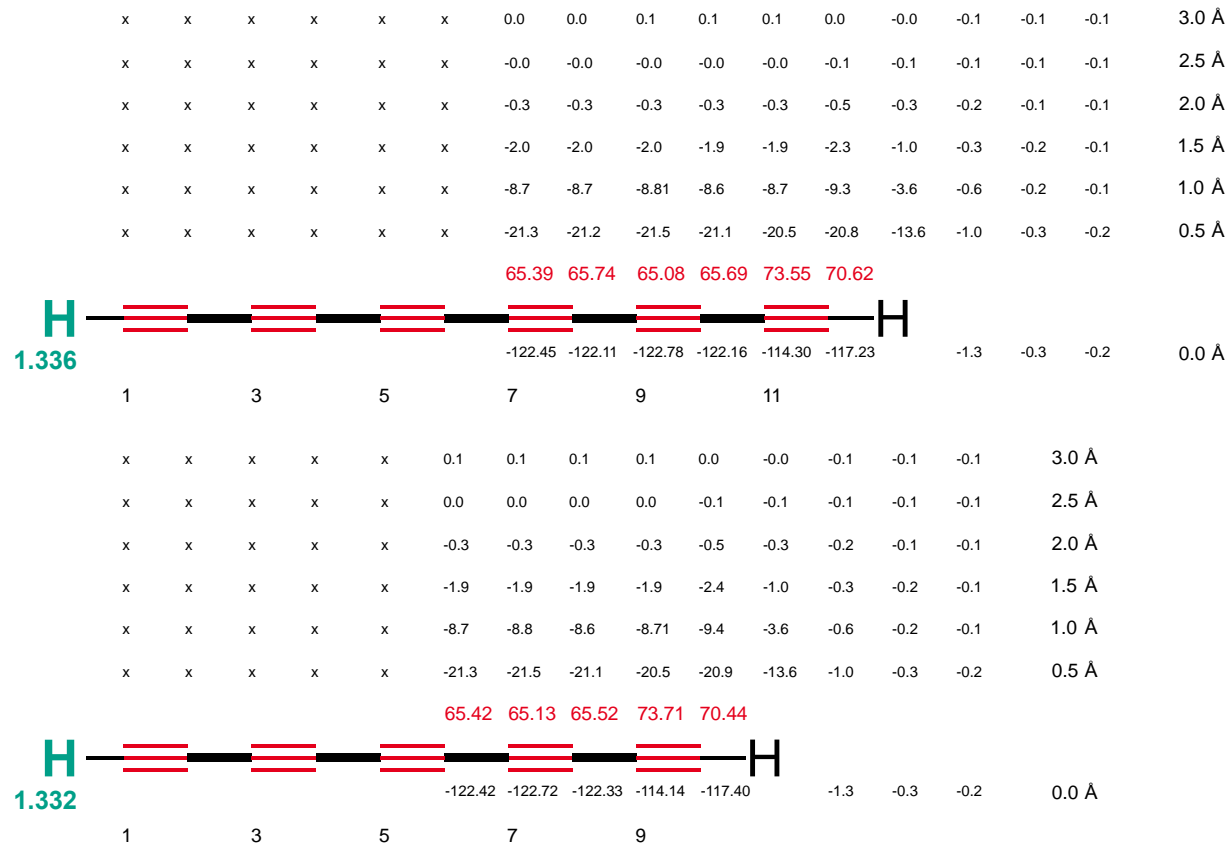


Figure s4-c. NICS grid plot for $\text{H}(\text{C}\equiv\text{C})_n\text{H}$ ($n = 6, 5$).

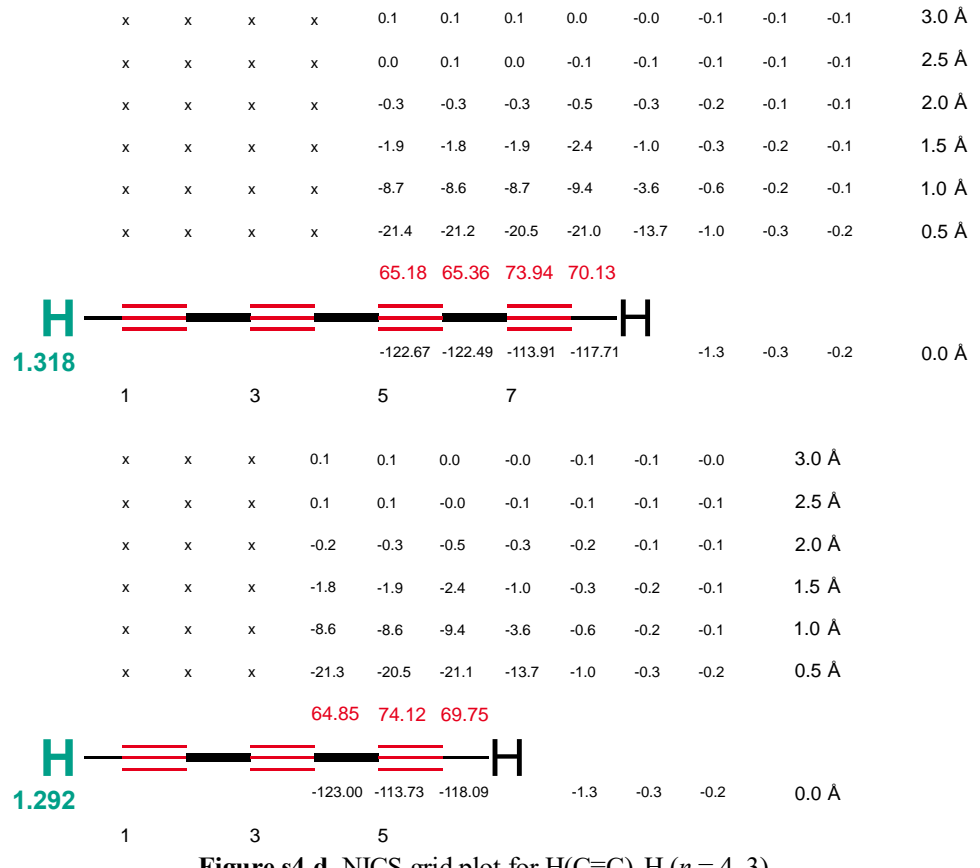


Figure s4-d. NICS grid plot for $\text{H}(\text{C}\equiv\text{C})_n\text{H}$ ($n = 4, 3$).

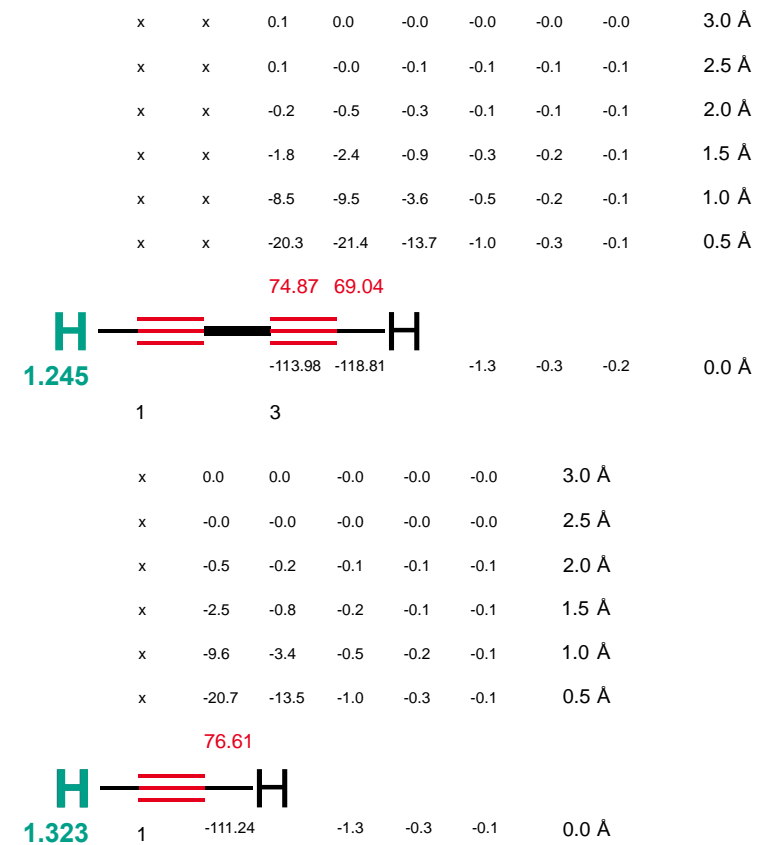


Figure s4-e. NICS grid plot format for $\text{H}(\text{C}\equiv\text{C})_n\text{H}$ ($n = 2, 1$).

Table s2. Carbon-carbon bond distances (\AA) in optimized structures of $\text{H}(\text{C}\equiv\text{C})_8\text{H}$ using nine different functionals compared to experimentally determined values in $t\text{-Bu}(\text{C}\equiv\text{C})_8t\text{-Bu}$.

functional:	experimental data	B3LYP		CAM-B3LYP		BLYP		BP86		BMK		PBE0		M06		M06L		ω B97xd		
C1-C2	N/A	1.208	N/A	1.211	N/A	1.201	N/A	1.225	N/A	1.227	N/A	1.205	N/A	1.210	N/A	1.207	N/A	1.215	N/A	1.204
C2-C3	1.367	N/A	1.350	N/A	1.3621	N/A	1.345	N/A	1.344	N/A	1.361	N/A	1.350	N/A	1.354	N/A	1.340	N/A	1.363	N/A
C3-C4	N/A	1.210	N/A	1.224	N/A	1.209	N/A	1.242	N/A	1.243	N/A	1.216	N/A	1.222	N/A	1.217	N/A	1.229	N/A	1.211
C4-C5	1.352	N/A	1.337	N/A	1.352	N/A	1.330	N/A	1.328	N/A	1.350	N/A	1.338	N/A	1.342	N/A	1.326	N/A	1.355	N/A
C5-C6	N/A	1.218	N/A	1.228	N/A	1.212	N/A	1.248	N/A	1.250	N/A	1.219	N/A	1.227	N/A	1.221	N/A	1.235	N/A	1.214
C6-C7	1.349	N/A	1.333	N/A	1.350	N/A	1.324	N/A	1.323	N/A	1.347	N/A	1.334	N/A	1.339	N/A	1.321	N/A	1.352	N/A
C7-C8	N/A	1.213	N/A	1.230	N/A	1.213	N/A	1.251	N/A	1.252	N/A	1.220	N/A	1.228	N/A	1.222	N/A	1.237	N/A	1.214
C8-C9	1.353	N/A	1.332	N/A	1.349	N/A	1.323	N/A	1.321	N/A	1.346	N/A	1.333	N/A	1.338	N/A	1.319	N/A	1.352	N/A
C9-C10	N/A	1.213	N/A	1.230	N/A	1.213	N/A	1.251	N/A	1.252	N/A	1.220	N/A	1.228	N/A	1.222	N/A	1.237	N/A	1.214
C10-C11	1.352	N/A	1.333	N/A	1.350	N/A	1.324	N/A	1.323	N/A	1.347	N/A	1.334	N/A	1.339	N/A	1.321	N/A	1.352	N/A
C11-C12	N/A	1.214	N/A	1.228	N/A	1.212	N/A	1.248	N/A	1.250	N/A	1.219	N/A	1.227	N/A	1.221	N/A	1.235	N/A	1.214
C12-C13	1.355	N/A	1.337	N/A	1.352	N/A	1.330	N/A	1.328	N/A	1.350	N/A	1.338	N/A	1.342	N/A	1.326	N/A	1.355	N/A
C13-C14	N/A	1.207	N/A	1.224	N/A	1.209	N/A	1.242	N/A	1.243	N/A	1.216	N/A	1.222	N/A	1.217	N/A	1.229	N/A	1.211
C14-C15	1.366	N/A	1.350	N/A	1.362	N/A	1.345	N/A	1.344	N/A	1.361	N/A	1.350	N/A	1.354	N/A	1.340	N/A	1.363	N/A
C15-C16	N/A	1.196	N/A	1.211	N/A	1.201	N/A	1.225	N/A	1.227	N/A	1.205	N/A	1.210	N/A	1.207	N/A	1.215	N/A	1.204
bond type:	C-C	C≡C	C-C	C≡C	C-C	C≡C	C-C	C≡C	C-C	C≡C	C-C	C≡C	C-C	C≡C	C-C	C≡C	C-C	C≡C	C-C	
average:	1.355	1.212	1.212	0.943	1.354	1.209	1.332	1.242	1.331	1.243	1.352	1.216	1.339	1.222	1.345	1.217	1.328	1.229	1.357	1.211
deviation from exp. data (%):	1.249	1.270	0.064	0.246	1.753	2.387	1.859	2.507	0.226	0.278	1.152	0.820	0.799	0.404	2.044	1.416	0.101	0.093		
sum of deviation from exp. (%):	2.15		0.31		4.14		4.37		0.50		1.97		1.20		3.46		0.19			

Table s3. The effect of basis set on NICS values at three distances from the centers of the C1 and C2 atoms of H(C≡C)₄H using the CAM-B3LYP functional.

basis set	6-311++G(d,p)		6-311+G(d)		6-311+G		6-31+G(d)	
	C1	C2	C1	C2	C1	C2	C1	C2
NICS (3.0 Å)	0.1	0.0	0.0	0.1	0.0	0.1	0.0	0.1
NICS (2.0 Å)	-0.5	-0.3	-0.5	-0.3	-0.5	-0.3	-0.4	-0.2
NICS (1.0 Å)	-9.4	-8.7	-9.4	-8.6	-9.5	-8.9	-9.4	-8.6

Table s4. The effect of functional on NICS values at three distances from the centers of the C1 and C2 atoms of H(C≡C)₄H using the 6-311++G(d,p) basis set.

functional	B3LYP		CAM-B3LYP		BLYP		BP86		BMK		PBE0		M06		M06L		ωB97xd	
	C1	C2	C1	C2	C1	C2	C1	C2	C1	C2	C1	C2	C1	C2	C1	C2	C1	C2
NICS (3.0 Å)	0.0	0.1	0.0	0.1	0.0	0.1	0.0	0.1	0.0	0.1	0.0	0.1	0.0	0.1	0.0	0.1	0.0	0.1
NICS (2.0 Å)	-0.5	-0.3	-0.5	-0.3	-0.5	-0.3	-0.5	-0.3	-0.5	-0.3	-0.5	-0.3	-0.5	-0.3	-0.5	-0.3	-0.5	-0.3
NICS (1.0 Å)	-9.3	-8.7	-9.3	-8.7	-9.3	-8.6	-9.3	-8.6	-9.3	-8.7	-9.3	-8.7	-9.3	-8.7	-9.3	-8.6	-9.3	-8.7

Table s5. Summary of the ^1H and ^{13}C NMR chemical shifts for $\text{H}(\text{C}\equiv\text{C})_n\text{H}$ ($n = 1\text{-}10$). All isotropic values have been corrected using TMS and the GIAO method at the CAM-B3LYP/6-311++G(d,p) level. The TMS isotropic ^1H and ^{13}C values are 31.9766 and 187.8458, respectively.

<i>n</i>	C1	C2	C3	C4	C5	C6	C7	C8	C9	C10	C11	C12	C13	C14	C15	C16	C17	C18	C19	C20	1H	
10	71.054	73.463	66.140	64.857	66.293	65.119	66.102	65.411	65.924	65.683	65.683	65.924	65.410	66.102	65.119	66.293	64.857	66.140	73.463	71.054	1.360	
9	70.989	73.502	66.110	64.925	66.210	65.191	66.052	65.554	65.863	65.863	65.554	66.052	65.191	66.210	64.925	66.110	73.502	70.989			1.359	
8	70.916	73.414	65.875	64.904	66.090	65.252	65.831	65.564	65.564	65.831	65.252	66.090	64.904	65.875	73.414	70.916					1.352	
7	70.784	73.439	65.795	64.978	65.933	65.346	65.628	65.628	65.346	65.933	64.978	65.795	73.439	70.784							1.344	
6	70.616	73.550	65.688	65.080	65.741	65.399	65.399	65.741	65.080	65.688	73.550	70.616									1.336	
5	70.443	73.710	65.517	65.128	65.423	65.423	65.128	65.517	73.710	70.443											1.332	
4	70.134	73.940	65.359	65.177	65.177	65.359	73.940	70.134													1.318	
3	69.753	74.119	64.850	64.850	74.119	69.753																1.292
2	69.036	73.869	73.869	69.036																		1.245
1	76.606	76.606																				1.323

Table s6. Summary of optimized bond lengths (\AA) for $\text{H}(\text{C}\equiv\text{C})_n\text{H}$ ($n = 1\text{-}10$) at the CAM-B3LYP/6-311++G(d,p) level.

<i>n</i>	C-H	C1-C2	C2-C3	C3-C4	C4-C5	C5-C6	C6-C7	C7-C8	C8-C9	C9-C10	
10	1.06344	1.20160	1.36203	1.20982	1.35272	1.21251	1.35013	1.21341	1.34928	1.21372	1.34910
9	1.06344	1.20161	1.36207	1.20983	1.35278	1.21249	1.35022	1.21337	1.34945	1.21358	
8	1.06343	1.20161	1.36211	1.20981	1.35290	1.21245	1.35041	1.21323	1.34982		
7	1.06339	1.20161	1.36219	1.20978	1.35306	1.21233	1.35078	1.21290			
6	1.06328	1.20143	1.36187	1.20975	1.35382	1.21214	1.35200				
5	1.06333	1.20162	1.36273	1.20940	1.35410	1.21115					
4	1.06328	1.20147	1.36339	1.20868	1.35629						
3	1.60315	1.20098	1.36501	1.20662							
2	1.06307	1.19953	1.37210								
1	1.06337	1.19419									

References (the titles are given in the capitalization format in which they were published)

- (s1) **BMK**-functional: "Development of density functionals for thermochemical kinetics", Boese, D. A.; Martin, J. M. L. *J. Chem. Phys.* **2004**, *121*, 3405-3416.
- (s2) **M06**-functional: "The M06 suite of density functionals for main group thermochemistry, thermochemical kinetics, noncovalent interactions, excited states, and transition elements: two new functionals and systematic testing of four M06-class functionals and 12 other functionals", Zhao, Y.; Truhlar, D. G. *Theor. Chem. Acc.* **2008**, *120*, 215-241.
- (s3) **CAM-B3LYP**-functional: "A new hybrid exchange–correlation functional using the Coulomb-attenuating method (CAM-B3LYP)", Yanai, T.; Tew, P. D.; Handy, N. C. *Chem. Phys. Lett.* **2004**, *393*, 51-57.
- (s4) **ωB97XD**-functional: "Long-range corrected hybrid density functionals with damped atom–atom dispersion corrections", Chai, J.-D.; Head-Gordon, M. *Phys. Chem. Chem. Phys.* **2008**, *10*, 6615-6620.
- (s5) **PBE0**-functional: "Toward reliable density functional methods without adjustable parameters: The PBE0 model", Adamo, C.; Barone, V. *J. Chem. Phys.* **1999**, *110*, 6158-6170.
- (s6) **B3LYP**, **BLYP**, and **BP86** functionals: (a) "Density-functional exchange-energy approximation with correct asymptotic behavior", Becke, A. D. *Phys. Rev. A*, **1988**, *38*, 3098-3100. (b) "Density-functional thermochemistry. III. The role of exact exchange", Becke, A. D. *J. Chem. Phys.* **1993**, *98*, 5648-5652. (c) "Development of the Colle-Salvetti correlation energy formula into a functional of the electron density", Lee, C.; Yang, W.; Parr, R. G. *Phys. Rev. B*, **1988**, *37*, 785-789.
- (s7) **M06L**-functional: "A new local density functional for main-group thermochemistry, transition metal bonding, thermochemical kinetics, and noncovalent interactions", Zhao, Y.; Truhlar, D. G. *J. Chem. Phys.* **2006**, *125*, 194101-194118.
- (s8) **BP86**-functional: "Density-functional approximation for the correlation energy of the inhomogeneous electron gas", Perdew, J. P. *Phys. Rev. B*, **1986**, *33*, 8822-8824.
- (s9) Pople basis set reference for "**6-311G**". An addition of "d" adds polarization functions of *d*-type to C, "p" adds *p*-type polarization functions to C and H atoms. "+/++" indicates added diffuse functions: (a) "Contracted Gaussian basis sets for molecular calculations. I. Second row atoms, Z = 11-18", McLean, A. D.; Chandler, G. S.; *J. Chem. Phys.* **1980**, *72*, 5639-5648. (b) "Self-consistent molecular orbital methods. XX. A basis set for correlated wave functions", Raghavachari, K.; Binkley, J. S.; Seeger, R.; Pople, J. A. *J. Chem. Phys.* **1980**, *72*, 650-654.
- (s10) Frisch, M. J.; Trucks, G. W.; Schlegel, H. B.; Scuseria, G. E.; Robb, M. A.; Cheeseman, J. R.; Scalmani, G.; Barone, V.; Mennucci, B.; Petersson, G. A.; Nakatsuji, H.; Caricato, M.; Li, X.; Hratchian, H. P.; Izmaylov, A. F.; Bloino, J.; Zheng, G.; Sonnenberg, J. L.; Hada, M.; Ehara, M.; Toyota, K.; Fukuda, R.; Hasegawa, J.; Ishida, M.; Nakajima, T.; Honda, Y.; Kitao, O.; Nakai, H.; Vreven, T.; Montgomery, J. A., Jr.; Peralta, J. E.; Ogliaro, F.; Bearpark, M.; Heyd, J. J.; Brothers, E.; Kudin, K. N.; Staroverov, V. N.; Kobayashi, R.; Normand, J.; Raghavachari, K.; Rendell, A.; Burant, J. C.; Iyengar, S. S.; Tomasi, J.; Cossi, M.; Rega, N.; Millam, J. M.; Klene, M.; Knox, J. E.; Cross, J. B.; Bakken, V.; Adamo, C.; Jaramillo, J.;

Gomperts, R.; Stratmann, R. E.; Yazyev, O.; Austin, A. J.; Cammi, R.; Pomelli, C.; Ochterski, J. W.; Martin, R. L.; Morokuma, K.; Zakrzewski, V. G.; Voth, G. A.; Salvador, P.; Dannenberg, J. J.; Dapprich, S.; Daniels, A. D.; Farkas, Ö.; Foresman, J. B.; Ortiz, J. V.; Cioslowski, J.; Fox, D. J. *Gaussian 09, Revision D.01*; Gaussian, Inc., Wallingford CT, 2009.

(s11) "tert-Butyl-End-Capped Polyynes: Crystallographic Evidence of Reduced Bond-Length Alternation", Chalifoux, W. A.; McDonald, R.; Ferguson, M. J.; Tykwinski, R. R. *Angew. Chem. Int. Ed.* **2009**, *48*, 7915-7919; "Polyine mit tert-Butyl-Endgruppen: kristallographischer Nachweis einer reduzierten Bindungslängenalternanz", *Angew. Chem.* **2009**, *121*, 8056-8060.

(s12) "Critical test of some computational methods for prediction of NMR ^1H and ^{13}C chemical shifts", Toomsalu, E.; Burk, P. *J. Mol. Model.* **2015**, *21*, 244-244.

(s13) Pople basis set reference for "**6-31G**". An addition of "d" adds polarization functions of *d*-type to C, "p" adds *p*-type polarization functions to C and H atoms. "+/++" indicates added diffuse functions: (a) "Self-Consistent Molecular-Orbital Methods. IX. An Extended Gaussian-Type Basis for Molecular-Orbital Studies of Organic Molecules", Ditchfield, R.; Hehre, W. J.; Pople, J. A. *J. Chem. Phys.* **1971**, *54*, 724-728. (b) "Self-Consistent Molecular Orbital Methods. XII. Further Extensions of Gaussian-Type Basis Sets for Use in Molecular Orbital Studies of Organic Molecules", Hehre, W. J.; Ditchfield, R.; Pople, J. A. *J. Chem. Phys.* **1972**, *56*, 2257-2261. (c), "The Influence of Polarization Functions on Molecular Orbital Hydrogenation Energies", Hariharan, P. C.; Pople, J. A. *Theor. Chem. Acc.* **1973**, *28*, 213-222. (d) "Accuracy of AH_n equilibrium geometries by single determinant molecular orbital theory", Hariharan, P. C.; Pople, J. A. *Mol. Phys.* **1974**, *27*, 209-214. (e) "THE ISOMERS OF SILACYCLOPROPANE", Gordon, M. S. *Chem. Phys. Lett.* **1980**, *76*, 163-168. (f) "Self-consistent molecular orbital methods. XXIII. A polarization-type basis set for second-row elements", Franch, M. M.; Pietro, W. J.; Hehre, W. J.; Binkley, J. S.; Gordon, M. S.; DeFrees, D. J.; Pople, J. A.; *J. Chem. Phys.* **1982**, *77*, 3654-3665. (g) "Compact Contracted Basis Sets for Third-Row Atoms: Ga-Kr", Binning, Jr. R. C.; Curtiss, L. A. *J. Comp. Chem.* **1990**, *11*, 1206-1216. (h) "Extension of Gaussian-2 (G2) theory to molecules containing third-row atoms K and Ca", Blaudeau, J.-P.; McGrath, M. P.; Curtiss, L. A.; Radom, L. *J. Chem. Phys.* **1997**, *107*, 5016-5021. (i) "6-31G* basis set for atoms K through Zn", Rassolov, V. A.; Pople, J. A.; Ratner, M. A.; Windus, T. L. *J. Chem. Phys.* **1998**, *109*, 1223-1229. (j) "6-31G* Basis Set for Third-Row Atoms", Rassolov, V. A.; Ratner, M. A.; Pople, J. A.; Redfern, P. C.; Curtiss, L. A. *J. Comp. Chem.* **2001**, *22*, 976-984.

(s14) "Ab initio calculation of the anisotropy effect of multiple bonds and the ring current effect of arenes—application in conformational and configurational analysis", Klod, S.; Klein-peter, E. *J. Chem. Soc., Perkin Trans. 2*, **2001**, 1893-1898.

(s15) "Nucleus-Independent Chemical Shifts (NICS) as an Aromaticity Criterion", Chen, Z.; Wannere, C. S.; Corminboeuf, C.; Puchta, R.; von Ragué Schleyer, P. *Chem. Rev.* **2005**, *105*, 3842-3888.

(s16) "Carbon rings: a DFT study on geometry, aromaticity, intermolecular carbon–carbon interactions and stability", Remya, K.; Suresh, C. H. *RSC Adv.* **2016**, *6*, 44261-44271.